



*Research article*

## **Application of intelligent X-ray image analysis in risk assessment of osteoporotic fracture of femoral neck in the elderly**

**Juan Du<sup>1,†</sup>, Junying Wang<sup>1,†</sup>, Xinghui Gai<sup>1</sup>, Yan Sui<sup>2</sup>, Kang Liu<sup>2</sup> and Dewu Yang<sup>1,\*</sup>**

<sup>1</sup> Department of Medical Technique, Beijing Health Vocational College, Beijing 102402, China

<sup>2</sup> Department of Radiology, Fuxing Hospital Affiliated with Capital Medical University, Beijing 100045, China

\* **Correspondence:** Email: 42819534@qq.com; Tel: +8618613310285.

† These two authors contributed equally.

**Abstract:** The paper focuses on establishing a risk assessment model of femoral neck osteoporotic fracture (FNOF) in the elderly population and improving the screening efficiency and accuracy of such diseases in specific populations. In literature research, the main risk factors of femoral neck osteoporosis (FNOP) in the elderly were studied and analyzed; the femur region of interest (ROI) and the hard bone edge segmentation model were selected from the X-ray digital image by using the image depth learning method. On this basis, the femoral trabecular score and femoral neck strength (FNS) in the set region were selected as the main evaluation elements, and the quantitative analysis method was established; an X-ray image processing method was applied to the feasibility study of FNOP and compared with dual-energy X-ray absorptiometry measurements of bone mineral density; Finally, the main risk factors of FNOP were selected and the prediction model of FNOP in the elderly population was established based on medical image processing, machine learning model construction and other methods. Some FNOP health records were selected as test samples for comparative analysis with traditional manual evaluation methods. The paper shows the risk assessment model of FNOF in the elderly population, which is feasible in testing. Among them, the artificial neural network model had a better accuracy (95.83%) and recall rate (100.00%), and the support vector machine prediction model had high specificity (62.50%). With the help of a machine learning method to establish the risk assessment model of FNOF for the elderly, one can provide decision support for the fracture risk assessment of the elderly and remind the clinic to give targeted interventions for the above high-risk groups in order to reduce the fracture risk.

**Keywords:** osteoporosis (OP); elderly patients; diagnosis; artificial intelligence; X-ray

---

## 1. Introduction

Osteoporosis (OP) is a degenerative disease with the decline of bone mineral density (BMD) with age. Clinically, it is often manifested as the loss of bone microstructure and the reduction of stress intensity, which readily lead to osteoporotic fracture (OF) and other complications. According to the literature statistics, there are nearly 200 million OP patients worldwide, and the incidence of complications is about 2.5 million people/year [1]. This is because the hip femoral neck has the particularity of supporting upper body weight, adjusting power transmission, participating in rotational abduction movement and so on. Meanwhile, femoral neck OF (FNOF) tends to occur in the middle-aged and elderly population, and its incidence rate has accounted for 51% [2]. About 25 and 20% of patients can have symptoms such as bone nonunion and femoral head necrosis [2]. With the intensification of global population aging and the extension of life expectancy, it has gradually become an important threat to the health of the elderly population.

The progress of femoral neck OP (FNOP) is concealed, and there is no obvious somatosensory representation. Patients can often detect it only after FNOF occurs. Once it occurs, it will not only prolong the rehabilitation cycle, but also increase the medical investment. After rehabilitation, FNOF patients' mobility will also be limited, greatly reducing the quality of life. Therefore, the establishment of screening and early intervention for FNOP high-risk groups is of great significance to achieve the primary prevention of FNOF in the elderly [3].

At present, OF risk assessment mainly focuses on the analysis of clinical medical diagnosis technology and the construction of a risk assessment model [4]. Among them, clinical medical diagnostic techniques mainly include a dual-energy X-ray absorptive BMD measurement method, quantitative ultrasound measurement method, quantitative magnetic resonance and bone physiological metabolism index analysis [5]. Because patients with OP usually have a decrease in BMD as the main indication, OF can occur when a large number of trabeculae are broken. Therefore, in 1994, the World Health Organization (WHO) used dual-energy X-ray absorptiometry (DXA) to measure the standard deviation between the BMD value and bone peak value of normal adults of the same sex and race as the diagnostic basis of OP [6]. In recent years, studies have shown that there are limitations of low sensitivity in evaluating the risk of OF based on BMD alone [7]. According to the cohort survey and clinical follow-up, the DXA method is used as the standard to predict the incidence that is much higher than the actual incidence. Meanwhile, the correlation between aging and the risk of occurrence is seven times that for BMD [8]. Finally, although the results of DXA measurement can reflect the risk of the elderly group due to the shortcomings of professional BMD testing equipment (e.g., high cost, low mobility and limited measurement factors), which has higher requirements for experienced diagnostic doctors and limits the scope of its screening application and promotion, it generally tends to be used as a means of clear diagnosis for patients. In the field of risk assessment model research, different scholars have studied by building a multifactor fracture risk assessment model, as shown in Table 1; it mainly includes the fracture risk assessment tool established by the University of Sheffield in the UK, which is based on age, femoral neck BMD and other fracture risk factors, and can be used to assess the risk of hip fracture in individuals aged 40–90 years within 10 years [9]. The prediction model has the advantages of simplicity, high sensitivity and strong fault tolerance, but it underestimates the

incidence probability of special populations such as postmenopausal women and persons with diabetes. Meanwhile, the model is established based on the natural incidence factors of the population and fails to consider the impact of human clinical intervention. The National Health and Medical Research Council (NHMRC) of Australia has built a 5/10-year risk assessment model for people over 60 years old [10]. Hippisley-Cox and Coupland established a risk assessment model for persons over 30 years old within 1–10 years based on the analysis of the medical records of British patients [11]. Berry et al. and Ioannidis et al. have established prediction tools for the elderly over 65 and 85 in long-term care institutions, respectively, trying to assess the risk under the condition of human intervention [12,13].

**Table 1.** Risk assessment model list for OF.

Research institutions	Model	Application population	Application field
The University of Sheffield	Fracture risk assessment tool	40–90 years old	Risk assessment within 10 years
NHMRC	Fracture displacement and reduction loss	60–96 years old	5/10-year of risk assessment
Hippisley-Cox and Coupland.	QFractureScores	Over 30 years old	Risk assessment within 1–10 years
Berry et al.	BMD	Over 65 years old	Risk assessment within 2 years in long-term care institutions in the United States of America
Ioannidis et al.	BMD	Over 85 years old	Risk assessment in long-term care institutions in Canada

Current research on risk assessment usually aims at identifying the overall fracture assessment needs of different populations, and the prediction lacks FNOF-targeted factors. At the same time, clinical medical diagnostic technology tends to be evaluated in combination with BMD measurements, and it highly depends on professional equipment such as bone densitometers and High Resolution CT, which reduces the popularity and intuition of OP and screening. Clinically, X-ray diagnosis has the advantages of low cost, strong specificity of bone imaging, simple operation and high popularity of equipment, especially the high definition of bone trabecula and periosteal structure imaging; it has become an important method of orthopedic diagnosis. However, the lack of quantitative analysis in X-ray testing has a high requirement for the clinical experience of diagnostic personnel, which has reduced the application scope of this technology in screening for a long time. In recent years, with the advancement of medical image processing technology and data processing hardware, image enhancement and intelligent analysis technology have been widely used in X-ray assisted diagnosis, which improves the efficiency of diagnosis and reduces the diagnostic errors caused by human factors [14]. Traditional medical image segmentation methods have some problems, such as low accuracy and poor adaptability. Therefore, many scholars have proposed a medical image segmentation method based on deep learning, which has achieved good practice results in medical image segmentation. An and Liu proposed a multilevel boundary-sensing RUNet segmentation model [15]. Shi et al. proposed a fuzzy active contour model based on a multi-channel convolutional neural network [16]. Therefore, based on the X-ray image processing method, the paper plans to build an auxiliary diagnosis model of FNOF

diseases in the elderly population, so as to improve the screening efficiency and performance of such diseases in specific populations.

## 2. Materials and method

The research contents of this paper are as follows. First, through literature research, we analyzed the main risk factors leading to FNOF in the elderly population. Second, using the image depth learning method, the region of interest (ROI) selection and hard bone edge segmentation model were established in the X-ray digital image. On this basis, the femoral trabecular bone score and femoral neck strength in the set region were selected as the main evaluation elements, and the quantitative analysis method was established. Third, an X-ray image processing method was applied to the feasibility study of FNOF and compared with DXA to measure BMD. Finally, we selected the main risk factors of FNOF, established the FNOF prediction model for the elderly based on medical image processing, constructed the machine learning model construction and other methods and selected some FNOF health records as test samples to compare with traditional manual evaluation, falls risks assessment tool and other models.

### 2.1. Analysis and selection of risk factors

#### 2.1.1. Analysis of FNOF risk factors

OP is usually characterized by decreased bone mass and degenerative changes in microstructure, which results in loose texture, reduced support strength, increased brittleness and high vulnerability to external forces. According to the research, the occurrence of OP is related to the patient's gender, race, family genetics, medication status, physical status (weight, height, exercise ability, etc.), nutritional status (occurrence of vitamin C, D, calcium, protein deficiency) and living habits (smoking, drinking, long-term caffeine drinking, physical activity frequency, etc.) [17]. Female patients are also closely related to menopause. At the same time, long-term use of steroids (such as glucocorticoids), anticoagulants (such as heparin), diuretics and/or anticonvulsants, or the occurrence of diabetes, thyroid dysfunction, cystinuria and/or other diseases also makes them prone to OP.

The occurrence of OP is the main cause of FNOF, but, at the same time, FNOF is affected by the quality and mechanical structure of the femoral neck itself. In the early stage, there are mainly phenomena such as bone mass reduction and bone microstructure degradation. Patients are vulnerable to external forces or sudden changes in daily activities. Among them, bone loss is mainly manifested by abnormal loss of the bone minerals and matrix. The degeneration of bone microstructure is manifested by the loose fracture of bone trabeculae. The patient's weight, history of falls, whether the hip joint is deformed (coxa vara or coxa valgus), history of hip joint trauma and other factors reflect the changes in the mechanical structure of the patient's hip joint. Generally, the greater the patient's weight, the greater the force on the femoral head, but some studies have shown that patients with heavier weight are usually stimulated by their own weight, and their bone mass is relatively more [18]. Therefore, it should be comprehensively evaluated in combination with their weight and patient bone mass. The femoral neck stem angle (FNSEA) refers to the angle between the longitudinal axis of the femoral shaft and the inner and lower parts of the femoral neck axis; it can affect the force transmission during exercise. It is normally between  $110^\circ$  and  $140^\circ$ , and can gradually decrease with age [19]. When

less than or greater than the normal range, it is manifested as coxa vara or coxa valgus, respectively, and thus changes the mechanical structure of the femoral neck; for example, hip varus can reduce the number of compressive and pressure-resistant bone trabeculae in the femoral neck, thereby increasing the hidden danger of FNOF.

### 2.1.2. Selection of FNOF assessment factors

Thirteen items were selected and included in the FNOF assessment factor set based on expert argumentation. As shown in Table 2, for the analysis of FNOF risk factors, gender, family genetic history of OP, body mass index (BMI), exercise ability, nutritional status, living habits, exercise habits, medication history, past medical history, fall history, development status, trauma history and femoral neck quality grade were selected as evaluation factors.

**Table 2.** Selection results for FNOF risk factors.

Element	Evaluation index	Value range
Gender		0: male; 1: premenopausal women; 2: postmenopausal women
Family genetic history of OP	Family genetic history of OP	0: No; 1: Yes
BMI	The ratio of weight to height squared	Actual calculation result
Exercise ability	Dyskinesia	0: No; 1: Yes
Nutritional status	Vitamin C, D, calcium, protein deficiency	0: No; 1: Yes
Living habits	Smoking, drinking or long-term caffeine drinking	0: No; 1: Yes
Exercise habits	Taking up manual job or maintaining an exercise habit	0: No; 1: Yes
Medication history	Long-term use of steroid hormones, anticoagulants, diuretics and anticonvulsants	0: No; 1: Yes
Past medical history	Suffering from diabetes, thyroid dysfunction, cystinuria and/or other disease(s)	0: No; 1: Yes
Fall history	Five related falls in the last 2 years	0: No; 1: Yes
Development status	Hip joint deformity	0: No; 1: Yes
Trauma history	History of hip joint trauma	0: No; 1: Yes
Femoral neck quality grade	Femoral neck compressive strength index	Actual calculation result

Among them, the sex factor can be used to indirectly reflect estrogen level; BMI was used to evaluate the compression degree of the femoral neck of the subjects. Exercise ability, fall history, motor system trauma history, hip joint development status, etc., reflect the subject's motor system development mechanism and previous injury status. The nutritional status, living habits and exercise habits were used to evaluate the bone development of subjects. Patients with vitamin C, D, calcium and/or protein deficiency are prone to bone demineralization and reduced bone density. Studies have

shown that long-term drinking and smoking can lead to BMD reduction [20]. However, regarding people who regularly drink coffee and soda for a long time, caffeine and carbonic acid intake tend to lead to an average 3.7% lower femur and tibia BMD and an average 5.4% lower BMD in the triangle area. Long-term use of steroid hormones, anticoagulants, diuretics and anticonvulsants has been recognized as a clinical risk for inducing OP. At the same time, clinical studies have shown that diabetes, thyroid dysfunction, cystinuria and other diseases are related to the occurrence of OP [21]. BMD, the compressive strength index (CSI) of femoral neck and bone geometric parameters are commonly used in clinical practice to reflect the quality grade of the femur. According to research reports, the CSI can comprehensively reflect the degree of OP of the femoral neck by integrating BMD and major bone geometric parameters, that is, the ability to resist fracture, so as to enable evaluation of the threshold of external force before fracture; it can improve the reliability of OP and prediction. Therefore, FNOF risk assessments need to combine the above multi-factor comprehensive assessment.

## 2.2. Femoral ROI and bony edge segmentation model

### 2.2.1. Image preprocessing

The data set in this paper adopts a DICOM file format, which is widely used in image storage and transmission in the field of medical imaging; it can contain photography and image information. In order to facilitate image analysis, we used the Pydicom toolkit to parse this format into the TIFF file format.

In the process of X-ray imaging, the contrast and spatial resolution of the image are reduced due to current noise, scattered noise, Gaussian noise, an uneven gray scale, blurred edges, patient body motion, light source size, detector nonlinearities and so on. In order to enhance the image quality, we adopted the improved hybrid wavelet filter denoising method, multi-scale image enhancement algorithm and dual-mode image reconstruction method to realize the functions of image noise removal, edge enhancement, contrast enhancement and resolution improvement, respectively. Among them, the improved hybrid wavelet filter denoising algorithm first reduces the current and scatter noise through image superposition and adaptive median filtering. Second, the image is decomposed by a dual-tree complex wavelet transform, the error is calculated based on the regional noise, the high-frequency wavelet coefficient is corrected according to the error and the quasi wavelet transform is implemented to complete the image reconstruction. The multi-scale image enhancement algorithm adopts multi-scale decomposition to obtain the image scale spectrum information, as well as high-frequency nonlinear transformation and low-frequency adaptive histogram equalization to improve the image contrast. The bimodal image reconstruction algorithm is based on a local contrast evaluation algorithm; it segments the image edge region; nonlinear mapping is carried out according to the high-frequency information of the image under edge and non-edge bimodal. After completion, a pseudo frequency domain transformation is carried out and the image is reconstructed. Pre-experiments showed that the dual-mode image reconstruction algorithm can enhance the image contrast and reduce the impact of tissue edge overlap.

### 2.2.2. Extraction of femoral ROI

The femur is an effective area for FNOF risk assessment. In order to eliminate the interference of

background and overlapping tissue and improve the efficiency of image processing, it is necessary to segment the image of the femur area. To date, some researches have applied recursive neural networks, residual networks and U-Nets to medical image segmentation. Our architecture adopts the U-Net network architecture with a recursive convolution layer and uses recursive residual unit as the basic neural unit. It not only has the advantages of fewer training samples, high accuracy and good noise resistance, but it also overcomes the network degradation problem in the iterative process of the deep neural network. The overfitting and underfitting problems are reduced, and the cyclic residual network can also realize feature optimization [22]. The method adopts the femur segmentation method based on U-Net (R2U-Net) network architecture. The specific steps are as follows.

X-ray images that meet the clinical diagnostic criteria for fracture were selected. The samples were respectively framed by the radiology diagnostic physician (5 years of experience) to select the femur area of the left and right legs, and the end position of the femoral neck was marked. The labeling information (i.e., femur framing coordinates and femoral head end coordinates) was generated into JSON files by the labeling software Labelbox, and the JSON information was analyzed to generate a label black-and-white mask image. Then, the image pixel matrix, JSON annotation information and label mask were mapped. Among them, there was no statistical difference in the professional title, age and professional ability assessment scores of diagnostic radiologists; the pre-experiment results were evaluated by senior physicians to meet the diagnostic criteria.

As shown in Figure 1, the R2U-Net was built on the basis of a U-Net network structure and consists of encoding, bridging and decoding. Among them, encoding was used to realize image encoding and feature extraction, bridging was used to realize path connection and decoding was used to restore image-encoded information to image pixel information. The three parts are composed of a convolution block and identification mapping. For our R2U-Net network, we substituted the convolution block with a recursive residual convolution block.

This module is composed of a recurrent residual convolutional layer, batch norm (BN) layer and PReLU activation layer. Identity mapping was used to connect the residual network. In the coding process, the recursive residual convolution layer reduces the size of the feature map via preset stepped convolution, so as to reduce the complexity of network operation. At the same time, setting the BN layer before activating the function can realize the uniform distribution of input. At the decoding layer, the high-level and low-level channel features are mapped into segmentation information through a  $1 \times 1$  convolutional and activation layer.

In this work, the sample image and label mask image are divided into  $120\ 572 \times 572$  image blocks for network training. The convolutional layer is used to extract image features, and the back-propagation network is used to optimize the model parameters based on the principle of minimizing error. A comparison of the manual segmentation model and intelligent segmentation is shown in Figure 2.

Thirty  $572 \times 572$  image blocks were used for the network test, and the performance of the model was verified by the test accuracy.

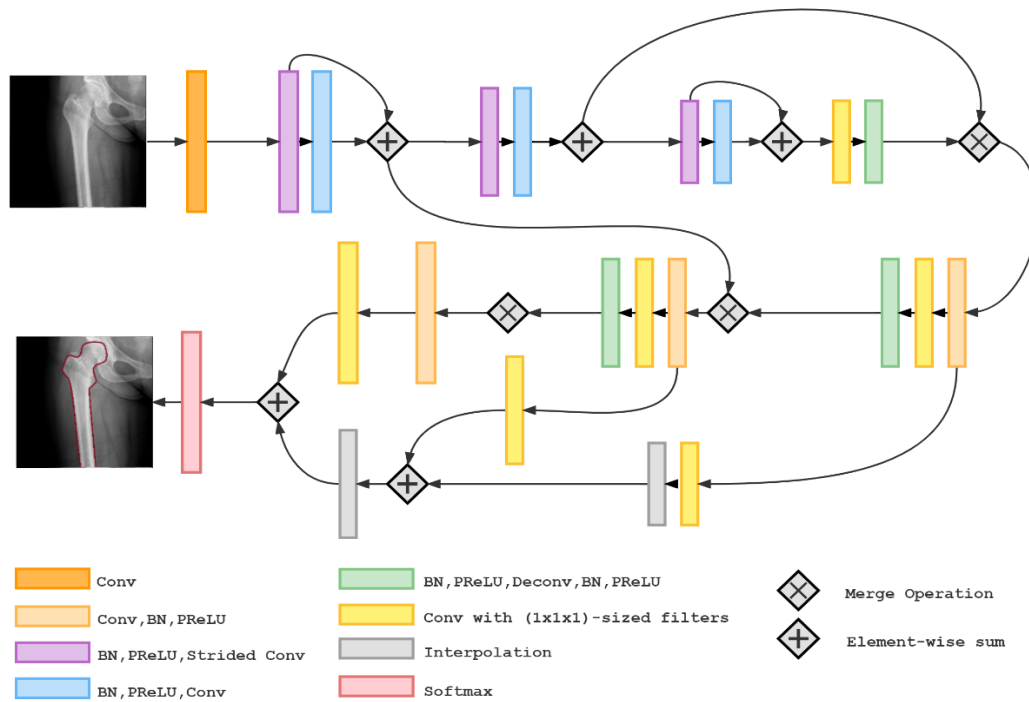


**Figure 1.** Construction process of R2U-Net network structure model.

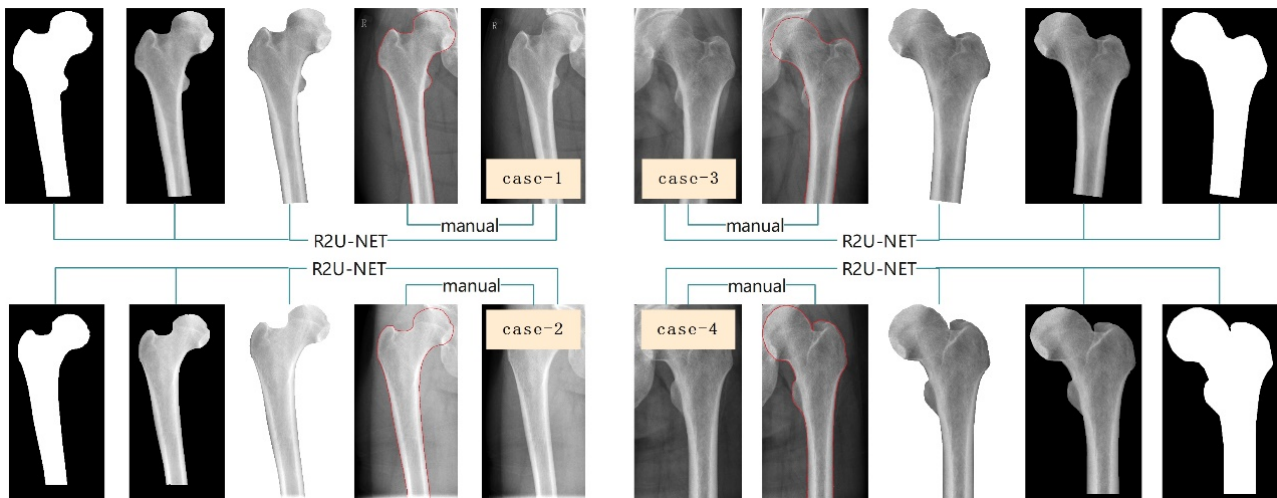


**Figure 2.** Model segmentation effect diagram.

*2.3. Pairwise registration*

In order to eliminate the morphological changes after femoral ROI segmentation, the thin plate spline registration method was used to adjust the femoral ROI formed after each independent segmentation to the standard coronal plane.

*2.4. Automatic calculation method of evaluation elements*

In this work, the graphic geometry method was used to realize the automatic calculation of the



CSI, FNSA and other evaluation elements. The specific methods are as follows.

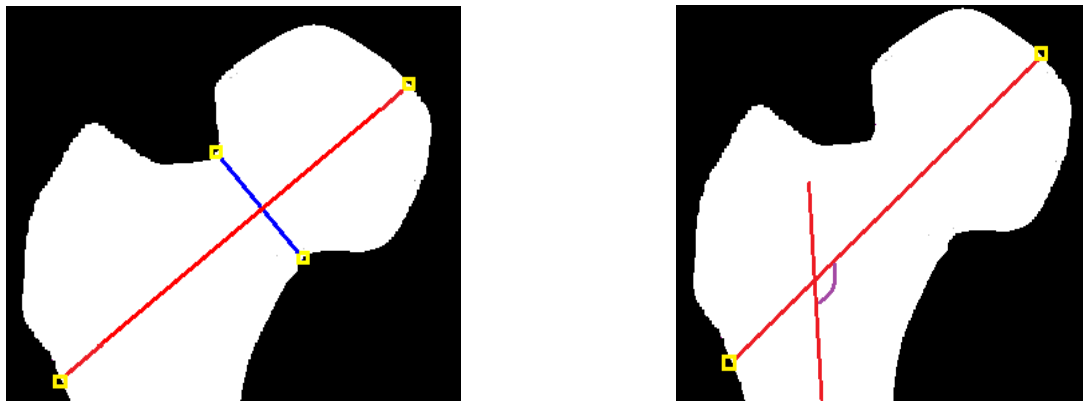
#### 2.4.1. CSI calculation

In this work, CSI was used to evaluate the femur quality grade, which is calculated based on Formula 1 on the basis of femur segmentation.

$$CSI = \frac{BMD \times FNW}{BW} \quad (1)$$

where FNW is the width of the femoral neck and BW is the weight of the patient.

As shown in Figure 3, we first established a straight-line sequence along the vertical direction of the hip axis, used the saddle point detection method to obtain the "saddle point" of the femoral neck contour and then selected the shortest line segment length through the "saddle point" to estimate the femoral neck width.



(a) Schematic diagram of femoral neck width measurement

(b) Schematic diagram of FNSA measurement

**Figure 3.** Schematic diagram of measurement of femoral geometry.

Image processing technology was used to extract the X-ray texture, and semi-quantitative indicators such as the trabecular bone and cortical bone thickness in texture were used to evaluate BMD according to Formula 2.

$$BMD \approx H_s \left( \sum_{i=0}^I \mu S(i) \right) \quad (2)$$

where  $H_s(x)$  is the mapping function between BMD and the gray value, and  $S(i)$  is the texture function of the X-ray block and  $\mu$  is the texture correction coefficient.

#### 2.4.2. FNSA calculation

We intersected the central axis of the lower edge of the femur with the axis of the hip joint and calculated the included angle of the two lines according to the coordinates to evaluate the FNSA value.

### 2.5. FNOF prediction model construction for the elderly

The FNOF prediction model for the elderly uses the factors shown in Table 2 as input variables, as well as machine learning models such as support vector machine (SVM), random forest, gradient-boosting decision tree (GBDT), AdaBoost, artificial neural network (ANN), XGBoost algorithms, etc., as modeling tools. Using the supervised learning results, SVM classifies the prediction data into positive and negative classes after calculating the hyperplane of the decision boundary. Random forests classify and output the predicted data through the use of multiple decision trees, and they are useful for both classification and regression tasks. GBDTs are a decision analysis algorithm that predicts data by iterating multiple regression trees, and a new tree is constructed by replacing residuals with gradients. Adaboost trains different classifiers for the same training set, sets weak classifiers and builds strong classifiers with better robustness. ANNs realize the repeated training and processing output of prediction data by constructing a complex network structure with a large number of interconnected processing units. Based on the gradient-boosting framework, XGBoost uses Newton's method to calculate the extreme value of the loss function.

## 3. Data analysis

### 3.1. Sample description

A total of 120 patients aged  $71 \pm 13.21$  years from July 2018 to September 2019 from the orthopedic outpatient department of Fuxing Hospital Affiliated with Capital Medical University were selected for the study, including 68 males and 52 females with a height of  $169.42 \pm 13.29$  cm and a weight of  $72.13 \pm 21.10$  kg. Sample exclusion conditions: 1) serious heart disease, hypertension, cardiovascular and cerebrovascular diseases or endocrine and metabolic diseases; 2) taking drugs that affect bone metabolism within 6 months; 3) there was no moderate or severe pain and limited movement in the affected side of the knee joint before injury; 4) no ankylosing spondylitis, rheumatoid arthritis and other diseases.

### 3.2. Detection method

For the control DXA, the Ge lunar iDXA scanner was used to measure the femoral neck and total hip BMD, and the lowest t value was selected to diagnose whether the subjects had OP.

The positive X-ray films of bilateral fixed knee joints and the corresponding diagnostic documents in which the X-ray films were stored in DICOM file format, has a total capacity of about 45.7 gb. The diagnostic document recorded the index diagnostic information of all X-ray films, including information on sclerosis, cyst, osteophytes, joint space distance, wear, tibial angle, femoral angle, tibial femoral angle and a series of indicators. The X-ray examination not only qualitatively evaluated BMD, but also the BMD with the help of semi-quantitative indicators such as trabecular bone and cortical bone thickness measurements.

## 4. Results

### 4.1. Extraction results for femoral ROI

Taking the manual segmentation by doctors as the standard, the R2U-NET model, gray threshold segmentation, gray co-occurrence matrix, region growth and Sobel algorithm were used to extract the ROI from the same 120 digital radiography images. The number of positive cases with a subjective evaluation difference of  $\leq 5\%$  was considered as the number of positive cases. A comparison of segmentation results is shown in Table 3. The segmentation accuracy of the R2U-NET model was 97.5%. The  $\chi^2$  test showed that there was no statistically significant difference between the two methods, but that there was a statistically significant difference between the two methods.

**Table 3.** Comparison of the segmentation effect of the R2U-NET; model and other segmentation effects (% , number of positive cases).

Group	n	Accuracy Rate	$\chi^2$	P
R2U-NET model segmentation	120	97.50 (117)	–	–
Manual segmentation	120	100.00 (120)	3.038	0.081
Gray threshold segmentation	120	87.50 (105)	8.649	0.003
Gray level co-occurrence matrix	120	88.33 (106)	7.660	0.006
Region growing algorithm	120	91.67 (110)	3.985	0.046
Sobel algorithm	120	90.00 (108)	5.760	0.016

### 4.2. Analysis results for femur quality grade

The texture characteristics of X-ray images of the femoral head were compared with the detection rate of OP in DXA. The DXA method adopted the WHO standard from 1994; the standard BMD peak value was used as the standard. When the t value  $\leq -2.5$  sd, OP was diagnosed;  $-1.0$  sd  $< -2.5$  sd is low bone mass, and a t value  $\geq -1$  sd is normal. As shown in Table 4, the correct rate of texture detection via X-ray imaging was 90.00%, which passes  $\chi^2$ . The difference with the DXA detection method is not statistically significant.

**Table 4.** Comparison of X-ray image texture and DXA OP detection rate results (% , number of positive cases).

Group	n	Accuracy Rate	$\chi^2$	P
X-ray image texture detection	120	90.00 (108)	2.1622	0.1414
DXA detection	120	95.00 (114)		

### 4.3. Test results for FNOF prediction model for the elderly population

Based on the clinical etiology, symptoms and imaging features of the patients, 120 samples were divided into fracture samples and normal samples after comprehensive evaluation by radiologists. At the same time, 120 samples were randomly divided into the training group and test group as 4:1, using test accuracy, specificity, recall and precision. As shown in Table 5, by constructing the FNOF

prediction model for the elderly population, it can be found that the ANN (the number of neurons in the hidden layer was 12, and Levenberg Marquardt was selected as the training function) had the highest test accuracy (95.83%) and recall rate (100.00%), and the SVM (the kernel function was a Gaussian kernel) prediction model had the highest specificity (62.50%) and a low prediction missed diagnosis rate.

**Table 5.** Detection results for prediction model.

Method	Test accuracy	Specificity	Recall	Precision
SVM <sup>1</sup>	91.67%	62.50%	70.83%	91.67%
Random Forest <sup>2</sup>	83.33%	50.00%	91.67%	83.33%
GBDT <sup>3</sup>	91.67%	58.33%	91.67%	87.50%
AdaBoost	87.50%	50.00%	91.67%	87.50%
ANN <sup>4</sup>	95.83%	58.33%	100.00%	95.83%
XGBoost	91.67%	54.17%	100.00%	91.67%

<sup>1</sup> Kernel function: mlp, mlp\_sigma: 0.5, method: sequential minimal optimization (SMO)

<sup>2</sup> n\_estimators: 400

<sup>3</sup> n\_estimators: 200

<sup>4</sup> Feedforward net: 12, trainFcn: Levenberg-Marquardt

## 5. Discussion

OP is a common physiological state of the elderly, making them prone to serious injuries such as fractures. In order to reduce the incidence of OP, it is necessary to accurately evaluate the status and risk factors of OP. At present, DXA is widely used in clinical practice to measure bone mineral content, but measuring bone mineral content alone has its limitations. This method cannot reflect bone structure and other factors, nor can it predict the risk of fracture [23]. With the deepening of research, a machine learning model related to multiple factors has been introduced into the evaluation of OP, that is, it fully considers the patient's individual environment, bone strength, external force on bone and other factors by building a prediction model, so as to reflect the current bone condition of the subjects and ensure that the subjects can be evaluated by the same standard. The occurrence of OP in the femoral neck is manifested by a change of anti-fracture ability and bone structure. Among them, the changes of anti-fracture ability were expressed by the CSI, including a decrease in the femoral neck width, an increase in stress and a decrease in femoral mineral volume. The decrease of bone mineral content was reflected by BMD. The increase in stress was manifested by weight gain, and the change of bone structure was realized as a change of FNSA.

## 6. Conclusions

DXA is a commonly used method to detect BMD for the diagnosis of OP, but, due to the high metabolic conversion rate of cancellous bone, the sensitivity of DXA diagnosis is reduced, resulting in limitations in the identification of cortical bone and cancellous bone. At the same time, DXA increases the measurement error due to high-density lesions, such as those caused by hyperosteogeny, articular disc degeneration, ligament ossification and vascular calcification, when measuring the lumbar spine in the forward position [24]. DXA measurement is also affected by factors such as the

living area and nationality of the tested individual, resulting in individual differences in bone shape, geometric size and bone peak value, which will also affect the accuracy of DXA measurement of BMD to a certain extent [25]. Based on the above problems, the research established X-ray diagnosis technology, as based on image processing technology, that has the characteristics of high X-ray imaging accuracy in bone trabecula and periosteum structures, established an image texture and bone density mapping model to evaluate the quality grade of the femoral neck and considered gender, family OP genetic history, BMI, exercise ability, nutritional status, living habits, exercise habits, medication history, past history, fall history and development status. The history of trauma and the quality grade of the femoral neck were found to be the influencing factors, and the machine learning method was used to establish the risk assessment model of FNOF for the elderly population. Through the tests with clinical cases, we found no statistical difference between the effect of femoral ROI segmentation and the effect of manual segmentation by doctors, and there was no statistical difference in the clinical detection rate compared with the traditional DXA detection method. FNOF resulted in higher prediction accuracy, and improved the work efficiency. The results show that the establishment of a risk assessment model for OF of the femoral neck in the elderly population using a machine learning method can provide decision support for fracture risk assessment in the elderly population to reduce the risk of fracture.

## Acknowledgments

The work was supported by the Vocational Education Teaching Reform Program of Beijing [2018-146].

## Conflict of Interest

The authors declare that there is no conflict of interest.

## References

1. S. Khosla, L. C. Hofbauer, Osteoporosis treatment: recent developments and ongoing challenges. *Lancet Diabetes Endocrinol.*, **5** (2017), 898–907. [https://doi.org/10.1016/s2213-8587\(17\)30188-2](https://doi.org/10.1016/s2213-8587(17)30188-2)
2. W. Chen, H. Lv, S. Liu, Bo Liu, Y. Zhu, X. Chen, et al., National incidence of traumatic fractures in China: a retrospective survey of 512187 individuals, *Lancet Glob. Health*, **5** (2017), 807–817. [https://doi.org/10.1016/s2214-109x\(17\)30222-x](https://doi.org/10.1016/s2214-109x(17)30222-x)
3. J. Compston, A. Cooper, C. Cooper, N. Gittoes, C. Gregson, N. Harvey, et al., UK clinical guideline for the prevention and treatment of osteoporosis. *Arch. Osteoporos.*, **12** (2017). <https://doi.org/10.1007/s11657-017-0324-5>
4. S. J. Curry, A. H. Krist, D. K. Owens, M. J. Barry, A. B. Caughey, K. W. Davidson, et al., Screening for osteoporosis to prevent fractures: US preventive services task force recommendation statement, *JAMA*, **319** (2018), 2521–2531. <https://doi.org/10.1001/jama.2018.7498>
5. E. M. Lewiecki, New and emerging concepts in the use of denosumab for the treatment of osteoporosis, *Ther. Adv. Musculoskelet. Dis.*, **10** (2018), 209–223. <https://doi.org/10.1177/1759720x18805759>

6. K. H. Rubin, S. Möller, T. Holmberg, M. Bliddal, J. Søndergaard, B. Abrahamsen, A new fracture risk assessment tool (FREM) based on public health registries, *J. Bone Miner. Res.*, **33** (2018), 1967–1979. <https://doi.org/10.1002/jbmr.3528>
7. Y. T. Lagerros, E. Hantikainen, K. Michaëlsson, W. Ye, H. Adami, R. Bellocco, Physical activity and the risk of hip fracture in the elderly: a prospective cohort study, *Eur. J. Epidemiol.*, **32** (2017), 983–991. <https://doi.org/10.1007/s10654-017-0312-5>
8. R. J. Valderrábano, J. Lee, L. Lui, A. R. Hoffman, S. R. Cummings, E. S. Orwoll, Older men with anemia have increased fracture risk independent of bone mineral density, *J. Clin. Endocrinol. Metab.*, **102** (2017), 2199–2206. <https://doi.org/10.1210/jc.2017-00266>
9. J. A. Kanis, C. Cooper, R. Rizzoli, J. Reginster, European guidance for the diagnosis and management of osteoporosis in postmenopausal women, *Osteoporos. Int.*, **30** (2019), 43–44. <https://doi.org/10.1007/s00198-018-4704-5>
10. N. Hollevoet, R. Verdonk, J. Kaufman, S. Goemaere, Osteoporotic fracture treatment, *Acta Orthop. Belg.*, **77** (2011), 441–447.
11. J. Hippisley-Cox, C. Coupland, Predicting risk of osteoporotic fracture in men and women in England and Wales: prospective derivation and validation of QFractureScores, *BMJ*, (2009). <https://doi.org/10.1136/bmj.b4229>
12. S. D. Berry, E. J. Samelson, M. J. Pencina, R. R. McLean, A. Cupples, K. E. Broe, et al., Repeat BMD screening and prediction of fracture, *JAMA*, **310** (2013), 1256–1262. <https://doi.org/10.1001/jama.2013.277817>
13. G. Ioannidis, A. Papaioannou, L. Thabane, A. Gafni, A. Hodsman, B. Kvern, et al., Family physicians' personal and practice characteristics that are associated with improved utilization of bone mineral density testing and osteoporosis medication prescribing, *Popul. Health Manag.*, **12** (2009). <https://doi.org/10.1089/pop.2008.0025>
14. J. C. Hyer, D. E. Deas, A. A. Palaiologou, M. E. Noujeim, M. J. Mader, B. L. Mealey, Accuracy of dental calculus detection using digital radiography and image manipulation, *J. Periodontol.*, **92** (2021), 419–427. <https://doi.org/10.1002/jper.19-0669>
15. F. An, J. Liu, Medical image segmentation algorithm based on multilayer boundary perception-self attention deep learning model, *Multimed. Tools Appl.*, **80** (2021), 15017–15039. <https://doi.org/10.1007/s11042-021-10515-w>
16. Q. Shi, S. Yin, K. Wang, L. Teng, H. Li, Multichannel convolutional neural network-based fuzzy active contour model for medical image segmentation, *Evol. Syst.*, **13** (2022), 535–549. <https://doi.org/10.1007/s12530-021-09392-3>
17. S. D. Berry, A. R. Zullo, Y. Lee, V. Mor, K. W. McConeghy, G. Banerjee, et al., Fracture Risk Assessment in Long-term Care (FRAiL): development and validation of a prediction model, *J. Gerontol. A Biol. Sci. Med. Sci.*, **73** (2018), 763–769. <https://doi.org/10.1093/gerona/glx147>
18. L. Shepstone, E. Lenaghan, C. Cooper, S. Clarke, R. Fong-Soe-Khioe, R. Fordham, Screening in the community to reduce fractures in older women (SCOOP): a randomised controlled trial, *Lancet*, **391** (2018), 741–747. [https://doi.org/10.1016/s0140-6736\(17\)32640-5](https://doi.org/10.1016/s0140-6736(17)32640-5)
19. N. Dagan, C. Cohen-Stavi, M. Leventer-Roberts, R. D. Balicer, External validation and comparison of three prediction tools for risk of osteoporotic fractures using data from population based electronic health records: retrospective cohort study, *BMJ*, (2017). <https://doi.org/10.1136/bmj.i6755>

20. G. E. Fuleihan, M. Chakhtoura, J. A. Cauley, N. Chamoun, Worldwide Fracture Prediction, *J. Clin. Densitom.*, **20** (2017), 397–424. <https://doi.org/10.1016/j.jocd.2017.06.008>
21. C. M. Rao, P. Singh, D. Maikap, P. Padhan, Musculoskeletal disorders in chronic obstructive airway diseases: a neglected clinical entity, *Mediterr. J. Rheumatol.*, **32** (2021), 118–123. <https://doi.org/10.31138/mjr.32.2.118>
22. M. Z. Alom, M. Hasan, C. Yakopcic, T. M. Taha, V. K. Asari, Recurrent residual convolutional neural network based on U-Net (R2U-Net) for medical image segmentation, preprint, arXiv:1802.06955.
23. Y. Su, J. Leung, T. Kwok, The role of previous falls in major osteoporotic fracture prediction in conjunction with FRAX in older Chinese men and women: the Mr. OS and Ms. OS cohort study in Hong Kong, *Osteoporos. Int.*, **29** (2018), 355–363. <https://doi.org/10.1007/s00198-017-4277-8>
24. H. Johansson, S. S. Dela, B. Cassim, F. Paruk, S. L. Brown, M. Conradie, et al., FRAX-based fracture probabilities in South Africa, *Arch. Osteoporos.*, **16** (2021), 51. <https://doi.org/10.1007/s11657-021-00905-w>
25. M. K. Skjødt, S. Möller, N. Hyldig, A. Clausen, M. Bliddal, J. Søndergaard, et al., Validation of the Fracture Risk Evaluation Model (FREM) in predicting major osteoporotic fractures and hip fractures using administrative health data, *Bone*, **147** (2021), 115934. <https://doi.org/10.1016/j.bone.2021.115934>



AIMS Press

©2023 author name, licensee AIMS Press. This is an open access article distributed under the terms of the Creative Commons Attribution License (<http://creativecommons.org/licenses/by/4.0>)